Communication

Context-Aware Statistical Dead Reckoning for Localization in IoT Scenarios

David Munoz-Rodriguez, Rafaela Villalpando-Hernandez *[ID] and Cesar Vargas-Rosales [ID]

Tecnologico de Monterrey, School of Engineering and Science, Monterrey 64849, Mexico;
dmunoz@itesm.mx (D.M.-R.); cvargas@tec.mx (C.V.-R.)
* Correspondence: rafaela.villalpando@tec.mx

Abstract: The current trends in 5G and 6G systems anticipate vast communication capabilities and the deployment of massive heterogeneous connectivity with more than a million internet of things (IoT) and other devices per square kilometer and up to ten million gadgets in 6G scenarios. In addition, the new generation of smart industries and the energy of things (EoT) context demand novel, reliable, energy-efficient network protocols involving massive sensor cooperation. Such scenarios impose new demands and opportunities to cope with the ever-growing cooperative dense ad hoc environments. Position location information (PLI) plays a crucial role as an enabler of several location-aware network protocols and applications. In this paper, we have proposed a novel context-aware statistical dead reckoning localization technique suitable for high dense cooperative sensor networks, where direct angle and distance estimations between peers are not required along the route, as in other dead reckoning-based localization approaches, but they are obtainable from the node's context information. Validation of the proposed technique was assessed in several scenarios through simulations, achieving localization errors as low as 0.072 m for the worst case analyzed.

Keywords: position location information; IoT; dead reckoning; stochastic dead reckoning; collaborative localization; context-aware localization

1. Introduction

Indoor and outdoor localization have re-gained relevance as an enabler of new applications and requirements introduced by IoT, EoT, Industry 4.0/5.0, and 5G/6G communications. For instance, the energy crisis has led to the EoT concept, which involves both industrial and domestic environments, as well as a widespread of smarter and more reliable scenarios in which energy consumption becomes a major issue and the deployment of energy-sensitive devices and systems will become even more relevant for static and dynamic applications.

Therefore, position location information (PLI) plays an important role in supporting the operation and management of mobile systems as it has become a crucial requirement for a growing and wide variety of location-based applications and services [1].

In scenarios where global navigation satellite systems (GNSS) are not available or their accuracy is compromised, most conventional position estimation systems consider a set of base stations as the reference sites, which are meant to have known locations, and they can be observed (or be seen) by a node of interest (NoI), whose coordinates need to be determined. In these scenarios, the node-to-landmarks distances can be estimated from a combination of parameters such as the received signal strength (RSS), time of arrival (ToA), time difference of arrival (TDoA), or angle of arrival (AoA) [2–4].

In ideal scenarios, simple range and angular observations may be sufficient to determine a 2D location. Those positioning setups are based on a direct observation of the radio source and are often referred to as single hop positioning systems. However, the presence of impairments precludes the operability of those systems, and several alternative trilateration schemes using multiple observation points are necessary.

In cases that lack a direct observation/connection and have limited power availability or unpredictable propagation scenarios, information delivery can be achieved via ad hoc node-to-node relays of transmitted information from/to, and many routing algorithms for node-to-node ad hoc paths selection can be found in the literature. Thus, PLI acquisition becomes cumbersome as conventional algorithms cannot be applied due to the lack of direct connectivity/observation.

This challenging problem becomes more relevant as the IoT and sensor networks become a pervasive experience, where densities as large as one million IP devices per square kilometer are anticipated for 5G and 6G systems.

In many cases, the device placement is imprecise, and it can be considered almost random; some probabilistic approaches have been suggested to support location acquisition processes, see [5–7].

The large number of IP devices, the mobility and connectivity changing scenarios, and the complexity of inhomogeneous propagation conditions cause uncertainty of the observable parameters. In order to have a reduced number of access points, low-cost alternative location techniques are demanded. Thus, context-aware information and collaborative location schemes have been suggested as promising techniques [8–11]. The use of cognitive approaches has also been suggested in order to acquire location information without a massive deployment of costly and bulky angle-range observation capabilities, and some relational schemes have also been proposed in the literature [12–14].

A dead reckoning approach usually depends on gyroscopic, accelerometer observations, the awareness of an initial reference location often called "a fix", and on the knowledge of the consecutive traveling direction finding [10] of the consecutive steps, as well as the range or path length in each travel direction, in order to determine the progress of a traveler at a given time. Thus, conventional dead reckoning approaches demand highly equipped nodes with accurate angle/distance measurement capabilities [15,16].

In the IoT scenarios where tiny sensor nodes are deployed, localization techniques based on the angle of arrival observations and range measurements, as well as the implied network communication and processing cost, might not be a feasible approach [17].

In the EoT context, fault/attack sensor detection and localization techniques for photovoltaic (PV) systems have been addressed using statistical signal processing combined with machine learning techniques; however, there is a high processing cost involved in the use of artificial intelligence (AI) approaches [18]. In addition to the computational cost, these methods are not scalable for high dense networks.

In Table 1, we present a broad comparison between the position location techniques discussed above. This table compares several approaches in terms of the expected accuracy, network infrastructure (e.g., node equipment cost), processing cost, and environment suitability.

Table 1. Location Techniques Comparison.

Principle	Network Infrastructure	Processing Cost	Scenario	Accuracy
Context-aware and collaboration location techniques [8–11].	Low equipped. Cognitive-based approaches, distance-based.	High	Low dense networks	Low
Relational-based approaches [12–14].	Low equipped ANs and nodes. Hop-count-based.	Low	High dense networks	Low
Dead Reckoning-based approaches [15,16].	High equipped ANs and nodes. Range/Angle-based.	High	High dense networks	High

As noted before, the methods in [15,16] are based on the dead reckoning principle. The method reported in [15] provides an accurate location estimation of the nodes in ad hoc networks, and the reported estimation error is around $[1.5 \times 10^{-2}$ to $3.5 \times 10^{-2}]$; however, they consider the time and angle of arrival estimation at each node in the route. Similarly, in [16], the authors propose a method based on previous measurements of the speed and acceleration of vehicles to calculate the current location using the dead reckoning approach; this implies that every vehicle in the network has measurement capabilities. The authors reported high location estimation errors.

In this paper, a novel dead reckoning approach based on the node context awareness and on the statistical characterization of the sensor node distribution is presented. The lack of the need for range/angle measurements equipment and processing makes the proposed technique adequate for the emerging localization paradigms. In this paper, we assume that source-to-destination node paths in a high-density scenario can be established. Nevertheless, the routing algorithm is unsubstantial for the purposes of this paper. Although the current technological trends include enhanced beam-forming capabilities [19], these are not required. However, at the initial point of an ad hoc path, we also show that the direction and range of successive steps can be obtained from the node distribution. The feasibility of the proposed algorithm is assessed in several scenarios in Section 3 based on Figures 4–7, where the accuracy of the method is evaluated under different network parameters, such as the node coverage range and node density.

Please note that the proposed method is partially based on examinations performed as part of thesis research work, as reported in [20].

2. Context-Aware Statistical Dead Reckoning Approach

In the case of Ad Hoc and Wireless Sensor Networks (AH-WSNs), direct connection between the NoI (node of interest) and base stations or anchor point (AP) may be unavailable. This lack of direct connectivity precludes the use of direct trilateration schemes. However, connectivity is established via the concatenation of consecutive links or hops. The localization of a NoI is obtained through the addition of successive vectors corresponding to the link hops. This demands that the hop lengths and physical directions be known [15,16].

APs are assumed to have fixed and known coordinates and they provide access to the rest of the telecommunication network. Several location and angular finding schemes for ad hoc scenarios have been proposed in the literature [21–26]. However, the reduced size, power availability constraints, and limited processing capabilities of most nodes make the deployment of direction-finding schemes unviable for the non-anchor nodes. In contrast, APs are assumed to have larger power budgets, higher reception sensitivity, and enhanced processing capabilities in order to be suited for direction finding deployment. In this paper, it is shown that context-aware information allows the application of dead reckoning techniques without a massive deployment of angle finding and direct range measurements, while in traditional schemes, such as those reported in [15,16], several distance/angle measurements are required.

The fast growth of sensor and ad hoc networks has already been noted, and this approach takes advantage of the large number of nodes deployed. In this paper, the proposed methodology is applicable for 2D scenarios; however, it can be generalized for 3D scenarios.

Let us consider a sensor network in which each node is aware of their one hop reachable nodes. Let n_i, $i = 1, 2, \ldots$, be a node with coordinates (x_i, y_i) and reachability radius R_i. We define an R_i-neighborhood or an R_i-ball, $\mathbf{B}(R_i)$ as the set of reachable nodes n_ζ with coordinates (x_ζ, y_ζ) within its coverage radius R_i; that is, $\mathbf{B}(R_i) = \{n_\zeta \mid (x_\zeta - x_i)^2 + (y_\zeta - y_i)^2 \leq R_i^2\}$. Note that the coverage range R_i is set by the sensitivity of the receiver/transmitter systems and transmitted power.

For an ordered sequence of nodes n_{i-1}, n_i, n_{i+1} in an ad hoc path, node n_i is meant to be reachable from both n_{i-1} and n_{i+1}, this is $n_i \in \mathbf{B}(R_{i-1}) \cap \mathbf{B}(R_{i+1})$, as illustrated in Figure 1. For known reachability radiuses R_{i-1} and R_{i+1}, the area A_{i-1}^{i+1} of the intersection of

$\mathbf{B}(R_{i-1})$ $\cap$ $\mathbf{B}(R_{i+1})$ is a function of the separation distance—$D_{i-1}^{i+1} = \sqrt{(x_{i-1} - x_{i+1})^2 + (y_{i-1} - y_{i+1})^2} = D_{i+1}^{i-1}$—of nodes n_{i-1} and n_{i+1}, and, as a matter of fact, it can be shown (see [27]) that these parameters relate, according to:

$$
\begin{aligned}
A_{i-1}^{i+1} &= f\left(D_{i-1}^{i+1}, R_{i-1}, R_{i+1}\right) \\
&= R_{i-1}^2 \left\{ arccos\left(\frac{\alpha}{2D_{i-1}^{i+1}R_{i-1}}\right) - \left(\frac{\alpha}{4D_{i-1}^{i+1^2}R_{i-1}^2}\right)\sqrt{4D_{i-1}^{i+1^2}R_{i-1}^2 - (\alpha)^2} \right\} \\
&+ R_{i+1}^2 \left\{ arccos\left(\frac{\gamma}{2D_{i-1}^{i+1}R_{i+1}}\right) - \left(\frac{\gamma}{4D_{i-1}^{i+1^2}R_{i+1}^2}\right)\sqrt{4D_{i-1}^{i+1^2}R_{i+1}^2 - (\gamma)^2} \right\},
\end{aligned}
\tag{1}
$$

where $\alpha = D_{i-1}^{i+1^2} + R_{i-1}^2 - R_{i+1}^2$ and $\gamma = D_{i-1}^{i+1^2} + R_{i+1}^2 - R_{i-1}^2$. Note that A_{i-1}^{i+1} in (1) is a monotonic function of the separation distance D_{i-1}^{i+1}. Therefore, for given reachability radiuses R_{i-1}, R_{i+1}, D_{i-1}^{i+1} can be inferred from A_{i-1}^{i+1}. As expressions involve transcendental functions, inversion becomes cumbersome, but it can be obtained numerically. In addition, note that for equal reachability radiuses, i.e., $R_{i-1} = R_{i+1}$, Equation (1) is reduced to:

$$
A_{i-1}^{i+1} = 2R_{i-1}^2 arccos\left(\frac{D_{i-1}^{i+1}}{2R_{i-1}}\right) - \frac{1}{2}D_{i-1}^{i+1}\sqrt{4R_{i-1}^2 - D_{i-1}^{i+1^2}},
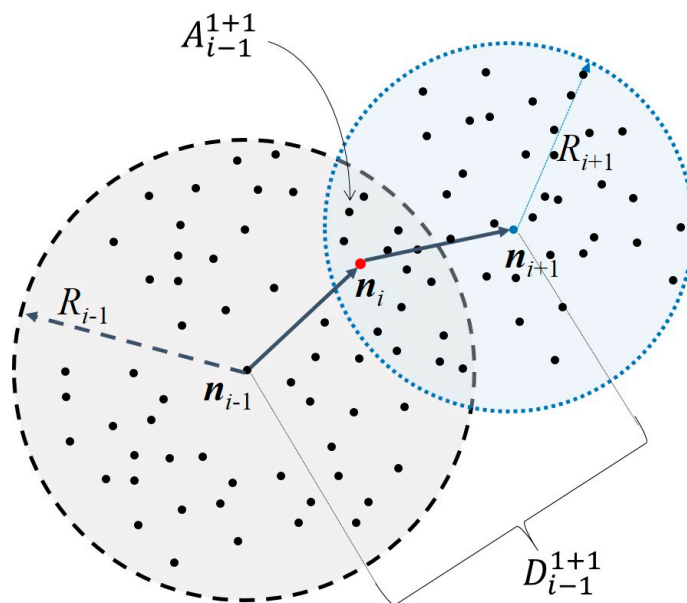\tag{2}
$$

Figure 1. Intersection of $\mathbf{B}(R_{i-1})$ with $\mathbf{B}(R_{i+1})$.

For instance, in a two-dimensional scenario, for the path segment n_{i-1}, n_i, n_{i+1}, D_{i-1}^i, and D_i^{i+1} denote, respectively, the separation of consecutive nodes—n_{i-1}, n_i, and n_i, n_{i+1}—that can be estimated from the field strength or delay measurements. On the other hand, nodes n_{i-1}, n_{i+1} are not adjacent, but their separation D_{i-1}^{i+1} can be inferred from A_{i-1}^{i+1} and, consequently, a triangle $\Delta(D_{i-1}^i, D_{i-1}^{i+1}, D_i^{i+1}) = {}_{i-1}\Delta_{i+1}$ can be defined by its side lengths, and such a triangle contains a segment n_{i-1}, n_i, n_{i+1} of a dead reckoning path that links an anchor to a NoI. A similar process can be conducted for nodes n_i, n_{i+1}, and n_{i+2}, and a triangle ${}_i^{i+1}\Delta_{i+2}$ can be constructed. In addition, it can be seen that side D_i^{i+1} is common to both triangles (see Figure 2).
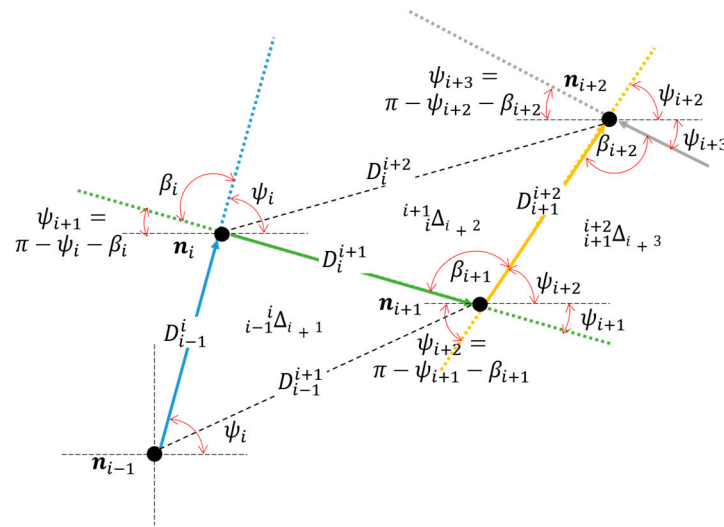
Figure 2. Construction of the Dead reckoning path from node n_{i-1} to node n_{i+2}.

Dead reckoning is the process of inferring a location using solely consecutive distances D_{i-1}^{i+1} and step direction estimates from a reference known site (x_0, y_0) or fix. Assuming the fix is at an anchor location (x_0, y_0) and that nodes n_i in a path occupy coordinates (x_i, y_i), $i = 1, 2, 3, \ldots$, the location of node n_n placed at (x_n, y_n) can be figured out as the vector addition $\rho = \sum_{i=1}^{n} \rho_i$, where $\rho_i = (\rho_i, \psi_i)$ is defined by $\rho_i = \sqrt{(x_i - x_{i-1})^2 + (y_i - y_{i-1})^2}$ and $\psi_i = \arctan \frac{y_i - y_{i-1}}{x_i - x_{i-1}}$ or $\psi_i = tan^{-1} \frac{y_i - y_{i-1}}{x_i - x_{i-1}}$, i.e., ρ_i is the range and ψ_i is the azimuthal angle. At this stage, coordinates (x_i, y_i) are unknown, with the exception of (x_0, y_0).

We pointed out that the range estimates ρ_i are obtainable through the field strength or delay measurements. However, angular observations tend to be bulkier and resource consuming. Nevertheless, anchor points are more able in terms of available energy, antenna capabilities, and computing power. Therefore, the initial angle ψ_0 is considered to be known and observable at the anchor point. The subsequent angular directions ψ_i, $i = 1, 2, \ldots$, are inferred from the node context as it is explained in the following paragraphs.

Recall that an ad hoc path is formed by consecutive hops connecting nodes n_0, $n_1, \ldots n_{i-1}$, n_i, n_{i+1}, n_{i+2}, $\ldots$, n_N. It can be observed that a path is contained within the sides of the concatenation of adjacent triangles $_0^1\Delta_2$, $_1^2\Delta_3$, $\ldots$, $_{i-1}^{i}\Delta_{i+1}$, $_{i}^{i+1}\Delta_{i+2}$, $\ldots$, $_{N-2}^{N-1}\Delta_N$ and the triangle concatenation allows the construction of a dead reckoning path.

Consider a homogeneous scenario with randomly deployed nodes to obtain A_{i-1}^{i+1}, which is the area estimation of the intersection of $\mathbf{B}(R_{i-1}) \cap \mathbf{B}(R_{i+1})$. The number N of nodes in an area A is distributed according to Poisson as $\frac{(\lambda A)^N}{N!} e^{-\lambda A}$, where λ stands for the node density (nodes per area) parameter, and for a given number N of nodes, the maximum probability occurs for $\lambda A = N$ [28]. Thus, for a known node density λ, the estimation of the area A_{i-1}^{i+1} can be obtained from the number N of nodes in the intersection $\mathbf{B}(R_{i-1}) \cap \mathbf{B}(R_{i+1})$.

In practice, the node density λ is not known, but it can be approximated from the average number of nodes N_{i-1} and N_{i+1} in balls $\mathbf{B}(R_{i-1})$ and $\mathbf{B}(R_{i+1})$, respectively. For instance, the estimated node density λ^* is given by: $\lambda^* \approx \left[\frac{N_{i-1}}{R_{i-1}^2} + \frac{N_{i+1}}{R_{i+1}^2} \right] / 4\pi$.

It has been stated that the location of all the nodes in the ad hoc path become known after the initial hop $n_0 - n_1$ is known, where n_0 is an anchor node with enhanced angle observation capabilities. Subsequent angular estimations can be obtained via the node context. Note that angle β_i subtended by adjacent hop lines of length D_{i-1}^{i} and D_i^{i+1} (see Figure 2) is given by:

$$\beta_i = \text{acos} \left[\frac{\left(D_{i-1}^i\right)^2 + \left(D_i^{i+1}\right)^2 - \left(D_{i-1}^{i+1}\right)^2}{2 D_{i-1}^i D_i^{i+1}} \right].$$ (3)

This scheme produces a vector sequence, $\rho_i = (\rho_i, \psi_i)$, which allows us to construct a dead reckoning path as the vector addition $\rho = n_0 + \sum_{i=1}^n \rho_i$, where node n_0 is meant to be an anchor node that has direction finding capabilities and known coordinates. Thus, $\rho_1 = (\rho_1, \psi_1)$ is known and the subsequent vectors $\rho_i = (\rho_i, \psi_i), i = 2, \ldots$, are defined by the measurements of $\rho_i = D_{i-1}^i$ and calculations $\psi_i = \pi - \psi_{i-1} - \beta_{i-1}$.

Note that for the triangle, $\Delta = \left(D_0^1, D_0^2, D_1^2\right)$, the placement of the edge D_0^1 is unique. However, there are two specular triangles with that common edge. This leads to two options for the location of n_2. This ambiguity grows as a spanning tree as the path progresses towards the node of interest NoI. Nevertheless, the uncertainties are removed by taking the intersection of the spanning trees with roots at different anchor points (see Figure 3).
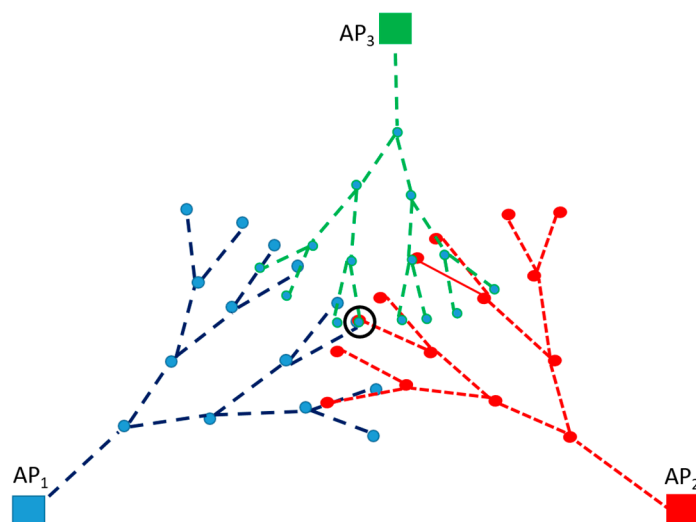

Figure 3. Intersection of spanning trees using dead reckoning paths.

Equation (1) states that $A_{i-1}^{i+1} = f\left(D_{i-1}^{i+1}, R_{i-1}, R_{i+1}\right)$. As it is a monotonic function of D_{i-1}^{i+1}, for given reachability radiuses R_{i-1} and R_{i+1}, D_{i-1}^{i+1} can be inferred from A_{i-1}^{i+1} through a minimization search function, given by:

$$\widetilde{D_{i-1}^{i+1}} = \min_{D_{i-1}^{i+1}} \left\{ \left[f\left(D_{i-1}^{i+1}, R_{i-1}, R_{i+1}\right) - A_{i-1}^{i+1} \right]^2 \right\},$$ (4)

Error drifts tend to accumulate along the path. Nevertheless, in this paper, it is shown that the multilateration of the reckoning paths allows for a location uncertainty reduction.

As stated previously, the proposed localization method can be extended for 3D scenarios. However, several considerations must be made. First, we will have the intersection of two spheres instead of circles (Figure 1). Second, distance D_{i-1}^{i+1} must be redefined to include the "z" coordinate. Third, this would force it to have an intersection volume, and Equations (1)–(3) would be reformulated for a 3D geometry. Additionally, the node density estimation equation must be reformulated under the basis of the intersection volumes. Finally, the minimization search function in Equation (4) must also be reformulated to perform the search on the intersection volume.

3. Simulations and Results

In order to assess the feasibility of the algorithm, different homogenous scenarios are created where the access points are assumed to be evenly spaced in a circle of radius R_A that defines the coverage area A. Note that $R_A = R_{i-1} = R_{i+1}$ for all i. The obtained location is compared to the actual NoI coordinates (x, y) by calculating the error according to $\varepsilon^2 = (x - x^*)^2 + (y - y^*)^2$. That is, we summarize the simulation process as follows:

1. For a given scenario, the number of nodes N_{i-1} and N_{i+1} within each of the coverage balls $\mathbf{B}(R_{i-1})$ and $\mathbf{B}(R_{i+1})$ corresponding to nodes n_{i-1} and n_{i+1} are known. Then, λ^* can be obtained.

2. Once λ^* is estimated and the number of nodes N at the intersection is known, it is possible to estimate the intersection area A_{i-1}^{i+1}.

3. From A_{i-1}^{i+1}, R_{i-1}, and R_{i+1}, we can calculate the estimated separation distance $\widetilde{D}_{i-1}^{i+1}$ using the minimization problem solution from (4).

4. Error will be assessed through a comparison of the estimated distance $\widetilde{D}_{i-1}^{i+1}$ versus the actual separation distance D_{i-1}^{i+1}.

5. We repeat this process depending on the number of hops required to reach the node of interest, NoI.

In the following simulations, we consider a scenario, such as in Figure 1, where the NoI is $n^* = n_i$. The accuracy (ε^2) of the proposed localization technique is evaluated for different node densities λ, coverage radiuses R_A, as well as for different separation distances D_{i-1}^{i+1}. Figure 4 shows the performance of the method under errors due to the difference in the current λ and the estimated λ^* node densities and to the difference between the true D_{i-1}^{i+1} and estimated $\widetilde{D}_{i-1}^{i+1}$ separation distances for $R_A = 3$ m.
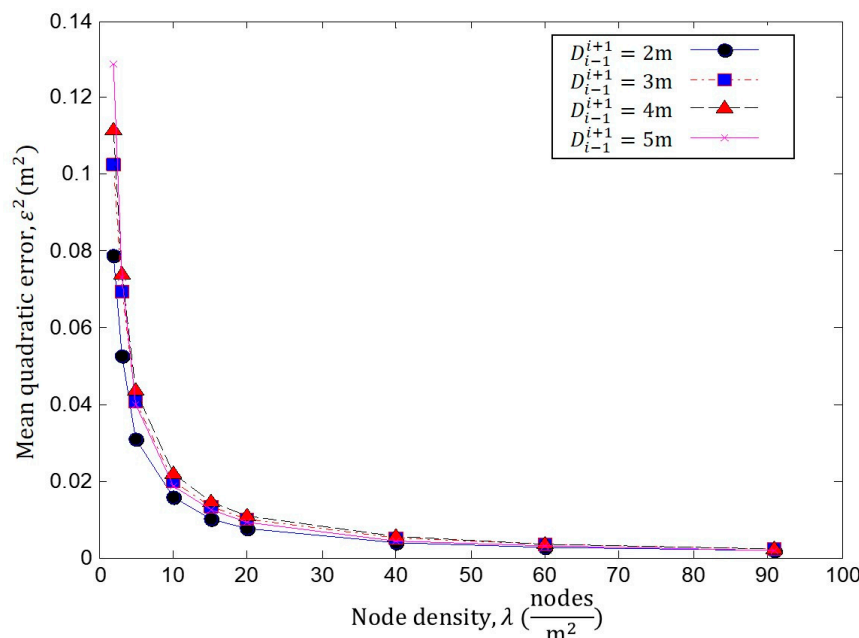

Figure 4. Performance analysis λ against ε^2 for different D_{i-1}^{i+1}, with $R_A = 3$ m.

In Figure 5, we compare the localization error ε^2 for different node densities $\lambda = (2, 3, 5, 10, 15, 20, 40, 60$ and $91)$ when $R_A = 3$. Each curve represents the localization error ε^2 at different separation distances D_{i-1}^{i+1}, ranging between 2 and 5 m. It is possible to observe how the error increases as the separation distance grows when the density is low. In addition, the error decreases due to the node density λ increments, as

these increments provide improvements in the intersection area. In Figure 6, we present the same results under a different perspective.
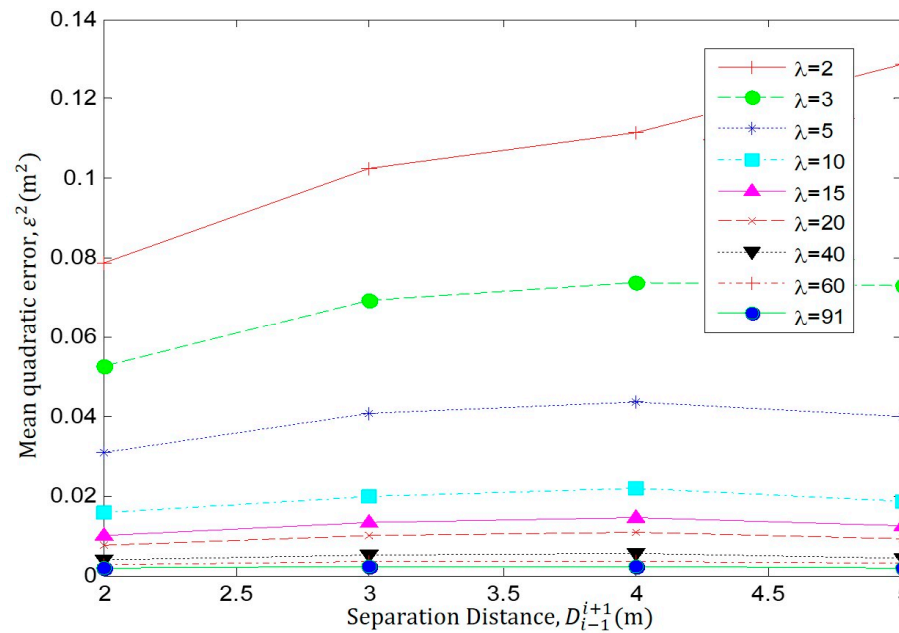

Figure 5. Performance analysis D_{i-1}^{i+1} against ε^2 for different λ, with $R_A = 3$ m.
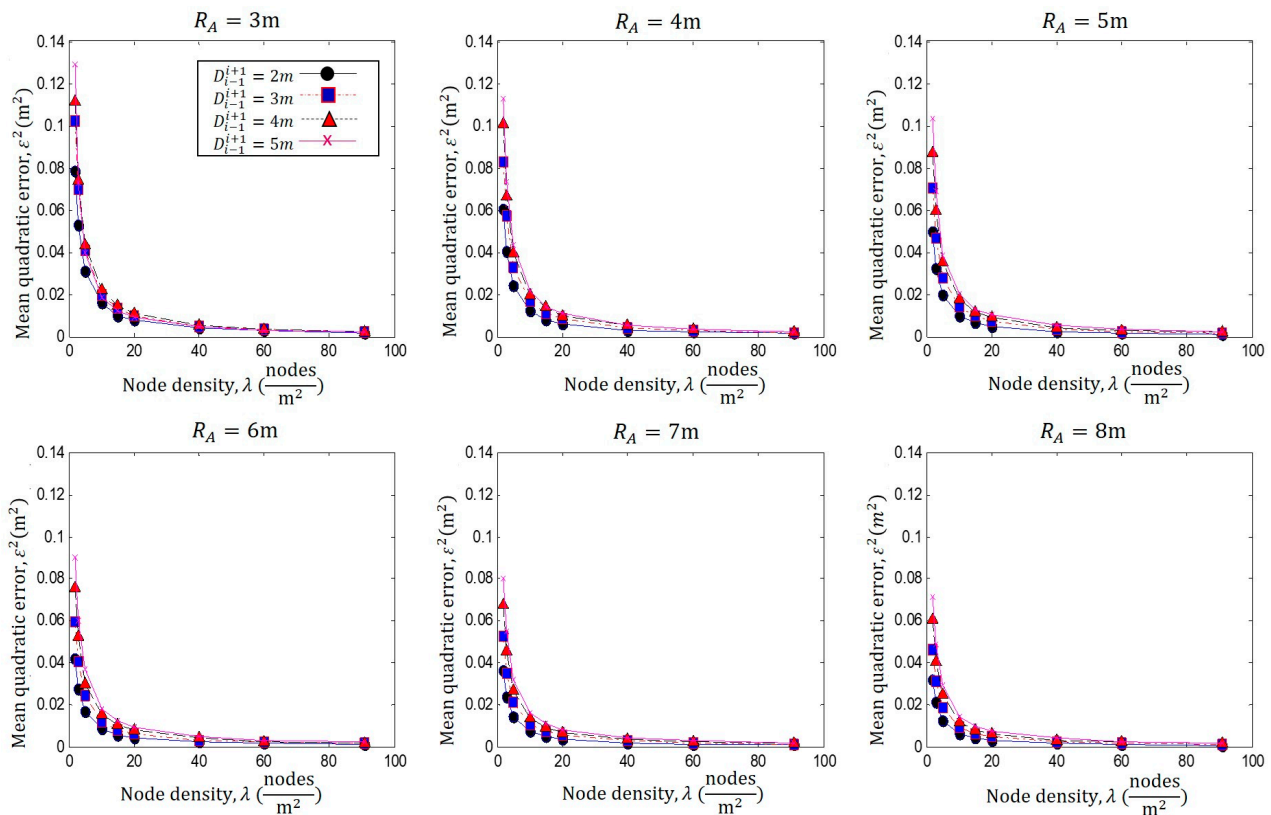

Figure 6. Performance analysis λ against ε^2 for different D_{i-1}^{i+1}, with $R_A = 3$ m to 8 m.

In Figure 5, it is clear that ε^2 decreases as increments of λ provide improvements in the estimation of the intersection area. In addition, ε^2 increases as D_{i-1}^{i+1} grows. These are the expected results, as the localization method depends on the estimated λ^* and

$\widetilde{D_{i-1}^{i+1}}$. Please note that despite the fact that the simulations are commanded to prove the true parameters (λ and D_{i-1}^{i+1}), the localization method estimates the NoI position using estimated parameters (λ^* and $\widetilde{D_{i-1}^{i+1}}$), as stated above.

In Figure 6, the same analysis is realized for several coverage ranges of R_A = 3 to 8 m, plotting the mean quadratic error ε^2 vs. λ. In this figure, we can observe that each of the graphs presents the same analysis as that in Figure 4, i.e., the localization error ε^2 increases as the separation distance D_{i-1}^{i+1} is increased.

However, it is also noticeable that as the size of the coverage radio R_A increases, the localization error ε^2 decreases. This is because the greater the intersection area, the greater the number of nodes at the intersection and the better the approximation; therefore, ε^2 is decreased.

In Figure 7, we present the same data representation as that in Figure 5 to provide a better understanding. From this data observation, it should be noted that the localization error ε^2 is inversely proportional to the coverage range R_A.
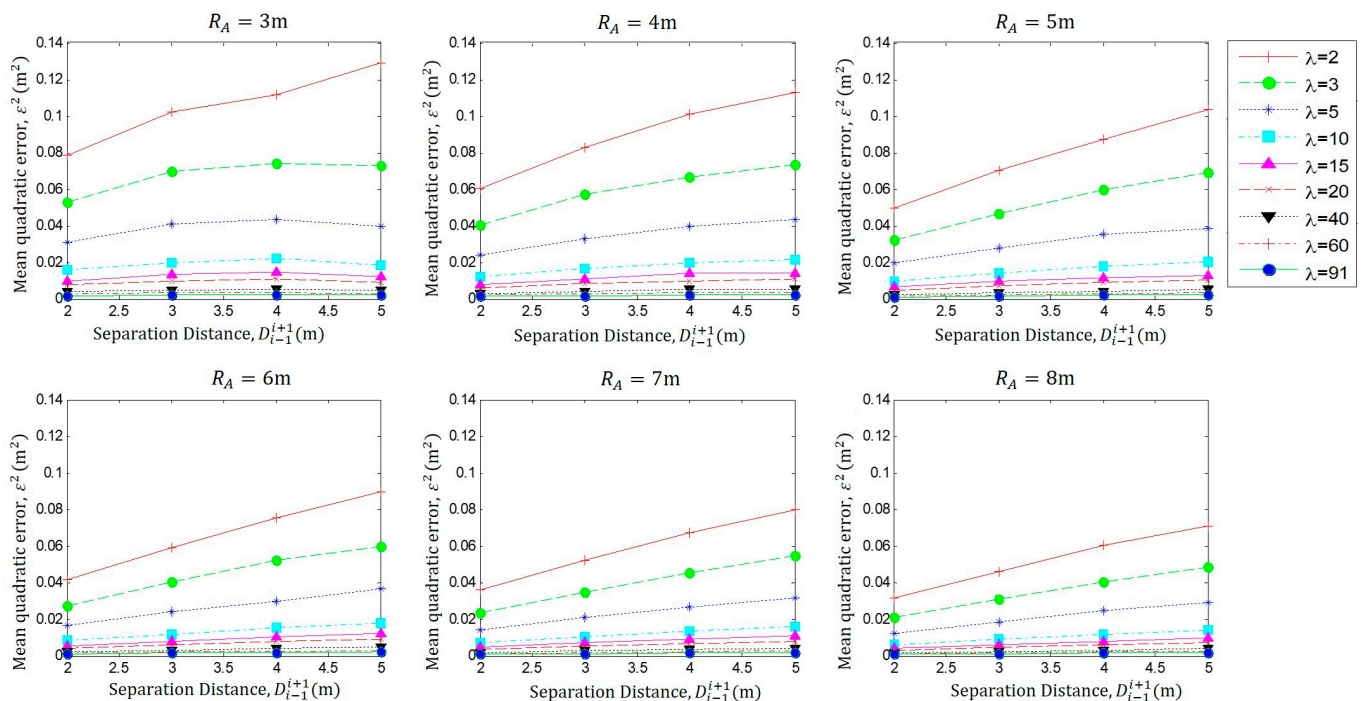
Figure 7. Performance analysis D_{i-1}^{i+1} against ε^2 for different λ, with R_A = 3 m to 8 m.

As we established earlier, dead reckoning does not require a large node density to obtain accurate results. However, if we compare the results, we can see that the decrease in the quality of the estimation is minimal between a low-density user scenario and a large-density one. It is also important to note that the last three values of user density appear to behave in the same way regardless of the size of the coverage range.

Please note that even though the initial consideration was for a scenario such as that illustrated in Figure 1, this methodology can be repeated for several hops to apply in scenarios such as that in Figure 3.

4. Conclusions

In this paper, it is shown that context information and the number of observable neighboring nodes allow the position location problem in dense ad hoc IoT scenarios to be solved without a high increase in the node's equipment. A stochastic dead reckoning methodology is presented and the proof of concept is demonstrated using simulations. The proposed algorithm estimates the local node density and constructs the feasible dead

reckoning paths that converge to determine the actual location of a NoI. Enhanced adequate processing and direction-finding capabilities are only required at anchor nodes, and these are not required for the remaining nodes that can estimate the lengths of the adjacent edges in the path from the field strength or delay measurements. This allows concatenations of triangles to be built that contain ad hoc paths that lead to the location inference of the NoIs. Performance results are reported for several scenarios, and it is shown that the proposed context-aware statistical dead reckoning method offers a good performance under several network conditions, such as coverage range, separation distance, and node density (i.e., $\varepsilon^2 < 0.072$ for worst case using a coverage range $R_i = 8$ m). The main achievements of the proposed method can be identified as follows:

- The method does not impose processing burn out on nodes.
- The method only requires angle measurement capabilities on anchor nodes.
- The method is based on easily obtainable network information (i.e., number of neighbors).
- The method provides an accuracy of $\varepsilon^2 = 0.13$ m and $\varepsilon^2 = 0.072$ m for $R_i = 3$ m and $R_i = 8$ m, respectively, for the worst cases analyzed.

Future analysis can be conducted for diverse network conditions and for randomly selected routes considering nodes with heterogeneous capabilities, including performance with non-uniform node densities.

References

1. Sujata, M.; Aruna, T.; Bikramaditya, D. An overview or a low energy UWB localization in IoT based system. In Proceedings of the International Symposium of Asian Control Association on Intelligent Robotics and Industrial Automation (IRIA), Goa, India, 20–22 November 2021.
2. Reza, Z.; Buehrer, R.M. *Handbook of Position Location. Theory, Practice and Advances*; Wiley-IEEE Press: Hoboken, NJ, USA, 2011.
3. Munoz-Rodriguez, D.; Bouchereau, L.F.; Vargas-Rosales, C.; Enriquez-Caldera, R. *Position Location Techniques and Applications*; Academic Press: Cambridge, MA, USA, 2009.
4. Brena, F.R.; García-Vázquez, J.P.; Galván-Tejada, C.; Muñoz-Rodriguez, D.; Vargas-Rosales, C.; Fangmeyer, J., Jr. Evolution of Indoor Positioning Technologies: A Survey. *J. Sens.* **2017**, *2017*, 1–22. [CrossRef]
5. Ramadurai, V.; Sichitiu, M.L. Localization in Wireless Sensor Networks: A Probabilistic Approach. In Proceedings of the International Conference on Wireless Networks, Las Vegas, NV, USA, 23–26 June 2003.
6. Abdallah, E.; Fevens, T.; Opatrny, J. Randomized 3D Position-Based Routing Algorithms for Ad-Hoc Networks. In Proceedings of the International Conference on Mobile and Ubiquitous Systems, San Jose, CA, 17–21 July 2006.
7. Wang, Y.; Yi, C.; Huang, M.; Li, F. Three-dimensional greedy routing in large-scale random wireless sensor networks. *Ad Hoc Netw.* **2013**, *11*, 1331–1344. [CrossRef]
8. Li, S.; Ni, W.; Sung, C.K.; Hedley, M. Recent advances on cooperative wireless localization and their application in inhomogeneous propagation environments. *Comput. Netw.* **2018**, *142*, 253–271. [CrossRef]

9.   Hwang, D.; Kim, S.; Kim, W.; Lee, B.; So, H. Cooperative localization considering estimated, location uncertainty in distributed ad hoc networks. *Int. J. Distrib. Sens. Netw.* **2018**, *14*, 1550147718759634.

10. Liu, Y.; Lu, S.; Liu, Y. COAL: Context Aware Localization for high energy efficiency in wireless networks. In Proceedings of the IEEE Wireless Communications and Networking Conference, Seattle, WA, USA, 21–25 March 2011.

11. Buehrer, R.M.; Wymeersch, H.; Vaghefi, R.M. Collaborative Sensor Network Localization: Algorithms and Practical Issues. *Proc. IEEE* **2018**, *106*, 1089–1114. [CrossRef]

12. Chen, S.; Chen, Y.; Trappe, W. Exploiting environmental properties for wireless localization and location aware applications. In Proceedings of the IEEE International Conference on Pervasive Computing and Communications, Hong Kong, 17–21 March 2008.

13. Perez-Gonzalez, V.; Munoz-Rodriguez, D.; Vargas-Rosales, C.; Torres-Villegas, R. Relational position location in ad-hoc networks. *Ad Hoc Netw.* **2015**, *24*, 20–28. [CrossRef]

14. Villalpando-Hernandez, R.; Munoz-Rodriguez, D.; Vargas-Rosales, C. Relational Positioning Method for 2D and 3D Ad Hoc Sensor Networks in Industry 4.0. *Appl. Sci.* **2021**, *11*, 8907. [CrossRef]

15. Hernandez, O.; Bouchereau, F.; Munoz, D. Maximum Likelihood Position Estimation in Ad-hoc Networks using a dead Reckoning Approach. *IEEE Trans. Wirel. Commun.* **2008**, *7*, 1572–1584. [CrossRef]

16. Zhang, M.; Yang, J.; Zhao, J.; Dai, Y. A Dead-Reckoning Based Local Positioning System for Intelligent Vehicles. In Proceedings of the IEEE International Conference on Power, Intelligent Computing and Systems (ICPICS), Shenyang, China, 12–14 July 2019.

17. Ghorpade, S.; Zennaro, M.; Chaudhari, B. Survey of Localization for Internet of Things Nodes: Approaches, Challenges and Open Issues. *Future Internet* **2021**, *13*, 210. [CrossRef]

18. Chen, L. *Signal Processing and Machine Learning Methods for Internet of Things: Smart Energy Generation and Robust Indoor Localization*; Columbia University: New York, NY, USA, 2022.

19. De Lima, C.; Didier, B.R.; Bourdoux, A.; Dardari, D.; Guillaud, M.; Isomursu, M. Convergent communication, sensing and localization in 6G systems: An overview of technologies, opportunities, and challenges. *IEEE Access* **2021**, *9*, 26902–26925. [CrossRef]

20. Roman, C.R. *Statistical Dead Reckoning for Ad Hoc Sensor Networks*; Master of Science in Electronic Engineering; Tecnologico de Monterrey: Monterrey, Mexico, 2014.

21. Peng, R.; Sichitiu, M.L. Angle of Arrival Localization for Wireless Sensor Networks. In Proceedings of the 3rd Annual IEEE Communications Society on Sensor and Ad Hoc Communications and Networks, Reston, VA, USA, 25–28 September 2006.

22. Niculescu, D.; Nath, B. Ad hoc positioning system (APS) using AOA. In Proceedings of the IEEE INFOCOM, San Francisco, CA, USA, 30 March–3 April 2003.

23. Nasipuri, A.; Li, K. A directionality based location discovery scheme for wireless sensor networks. In Proceedings of the ACM International Workshop on Wireless Sensor Networks and Applications, Atlanta, GA, USA, 28 September 2002.

24. Biswas, P.; Aghajan, H.; Ye, Y. Integration of angle of arrival information for multimodal sensor network localization using semidefinite programming. In Proceedings of the 39th Asilomar Conference on Signals, Systems and Computers, Pacific Grove, CA, USA, 1–5 November 2005.

25. Choi, S.; Sarabandi, K. 3-D direction finding using a single antenna. In Proceedings of the IEEE Antennas and Propagation Society International Symposium, Memphis, TN, USA, 6–11 July 2014.

26. Bojja, J.; Kirkko-Jaakkola, M.; Collin, J. Indoor Localization Methods Using Dead Reckoning and 3D Map Matching. *J. Signal Process. Syst.* **2014**, *76*, 301–312. [CrossRef]

27. Stoyan, D.; Stoyan, H. *Fractals, Random Shapes and Point Fields. Methods of Geometrical Statistics*; John Wiley: Hoboken, NJ, USA, 1994.

28. Williams, R.H. *Probability, Statistics and Random Processes*; Simon & Schuster: New York, NY, USA, 1971.